Crystallized White Dwarfs in Scalar-Tensor Gravity

Sofía Vidal Guzmán

Laboratory of Theoretical Physics,
University of Tartu

May 9, 2025

DOI: 10.1103/PhysRevD.111.084075
in collaboration with A. Wojnar, L. Järv, D. Doneva

Introduction

Properties & Motivation

- Final evolutionary stage of stars $M_* \lesssim 10 M_\odot$
- Extremely high densities $\rho \sim 10^6$ gcm^{-3}
- Electron degeneracy pressure prevents collapse
- "Simply" cools down during rest of its evolution
- Chandrasekhar limiting mass $\approx 1.4\ M_\odot$

- sub- and super-Chandrasekhar WD
- gravitational wave emission: binary systems or rotating massive WD with axisymmetry breaking

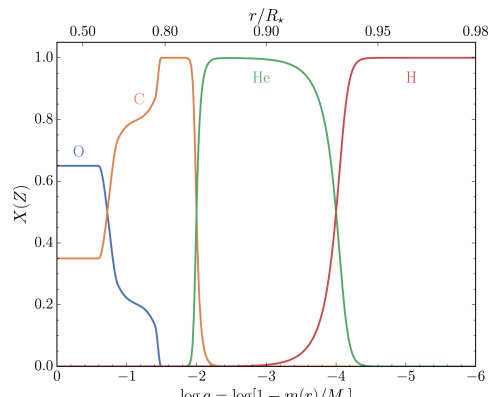

Figure 1. Fig. 1. Chemical layering in a representative model of a $0.6 M_\odot$ H-dominated atmosphere WD. The atmospheric layers, located at $q < -15$, are not shown here. By Saumon, Blouin, and Tremblay 2022.

Introduction

Hertzsprung-Russell Diagram

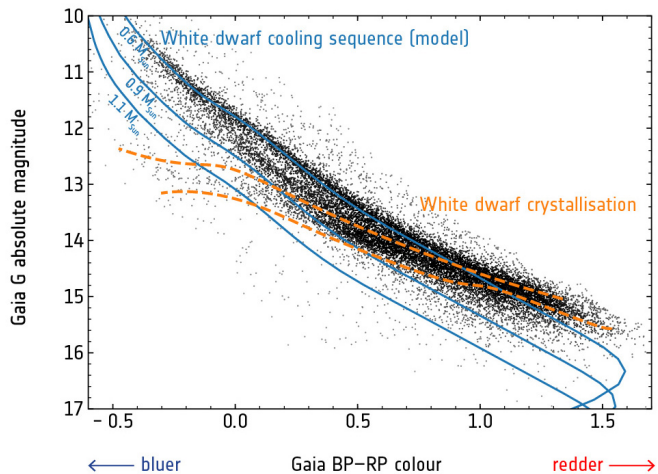

Figure 2. Observational Gaia color–magnitude Hertzsprung–Russell diagram for white dwarfs within 100 pc of the Sun. Taken from Tremblay et al. 2019.

Part I

Mass-Radius Relation

Mass-Radius Relation

Scalar-tensor Theory

- Action in Einstein frame

$$S = \frac{1}{16\pi G}\int \mathrm{d}^4x\sqrt{-g}\left[\tilde{R} - 2\tilde{g}^{\mu\nu}\tilde{\partial}_\mu\tilde{\varphi}\tilde{\partial}_\nu\tilde{\varphi} - V(\tilde{\varphi})\right] + S_\mathrm{m}\left(A^2(\tilde{\varphi})\tilde{g}_{\mu\nu}, \chi\right) \ , \tag{1}$$

- Field equations in Einstein frame with $\mathrm{d}\tilde{s}^2 = -\,\mathrm{e}^{2\tilde{\phi}(r)}\,\mathrm{d}t^2 + \mathrm{e}^{2\tilde{\Lambda}(r)}\,\mathrm{d}\tilde{r}^2 + \tilde{r}^2\mathrm{d}\Omega^2$

$$\frac{2\tilde{\Lambda}'}{\tilde{r}} = 8\pi G A^4(\tilde{\varphi})\rho\,\mathrm{e}^{2\tilde{\Lambda}} + \frac{1-\mathrm{e}^{2\tilde{\Lambda}}}{\tilde{r}^2} + \tilde{\varphi}'^2 + \frac{V(\tilde{\varphi})}{2}\,\mathrm{e}^{2\tilde{\Lambda}} \ , \tag{2}$$

$$\frac{2\tilde{\phi}'}{\tilde{r}} = 8\pi G A^4(\tilde{\varphi})p\,\mathrm{e}^{2\tilde{\Lambda}} - \frac{1-\mathrm{e}^{2\tilde{\Lambda}}}{\tilde{r}^2} + \tilde{\varphi}'^2 - \frac{V(\tilde{\varphi})}{2}\,\mathrm{e}^{2\tilde{\Lambda}} \ , \tag{3}$$

$$\tilde{\varphi}'' = \left[4\pi G\alpha A^4(\tilde{\varphi})(\rho - 3p) + \frac{1}{4}\frac{\mathrm{d}V}{\mathrm{d}\tilde{\varphi}}\right]\mathrm{e}^{2\tilde{\Lambda}} - \left(\tilde{\phi}' - \tilde{\Lambda}' + \frac{2}{\tilde{r}}\right)\tilde{\varphi}' \ , \tag{4}$$

$$p' = -(\rho + p)\left(\tilde{\phi}' + \alpha\tilde{\varphi}'\right) \tag{5}$$

- For a massive theory with

$$\alpha(\tilde{\varphi}) = \frac{\mathrm{d}\ln A(\tilde{\varphi})}{\mathrm{d}\tilde{\varphi}} = \alpha_0 \quad \text{and} \quad V(\tilde{\varphi}) = 2m_{\tilde{\varphi}}^2\tilde{\varphi}^2 \ . \tag{6}$$

Mass-Radius Relation

Chandrasekhar Equation of State

Describes pressure p and energy density ρ of a fully degenerate, relativistic gas

$$p(x) = \frac{\pi m_e^4 c^5}{3h^3}\left[(2x^3 - 3x)\sqrt{1+x^2} + 3\sinh^{-1} x\right] \tag{7a}$$

$$\begin{aligned}\rho(x) &= \rho_0 + \epsilon_{\text{kin}}/c^2 \\ &= \frac{8\pi\mu_e m_p (m_e c)^3}{3h^3}x^3 + \frac{3\pi m_e^4 c^3}{h^3}\left[(2x^3 + x)\sqrt{1+x^2} - \sinh^{-1} x\right]\end{aligned} \tag{7b}$$

where x is related to the the Fermi momentum p_F

$$x := \frac{p_F}{m_e c}$$

Electron mass m_e, mean molecular weight per electron μ_e, Planck's constant h, proton mass m_p, speed of light c

Mass-Radius Relation

Numerical Results

- ODE $\tilde{\Lambda}', \tilde{\phi}', \tilde{\varphi}'', p'$
- EOS $p(x), \rho(x)$
- Boundary conditions

$$\rho(\tilde{r} = 0) = \rho_c$$
$$\tilde{\Lambda}(\tilde{r} = 0) = 0$$
$$\tilde{\varphi}'(\tilde{r} = 0) = 0$$
$$\lim_{\tilde{r} \to \infty} \tilde{\varphi}(\tilde{r}) = 0$$

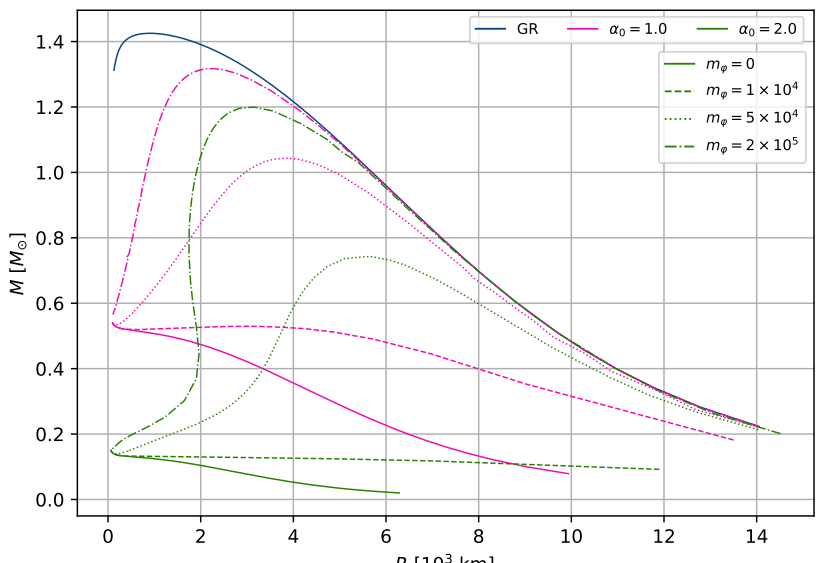

Figure 3. Mass-radius relation.

Mass-Radius Relation

Numerical Results – Density profile

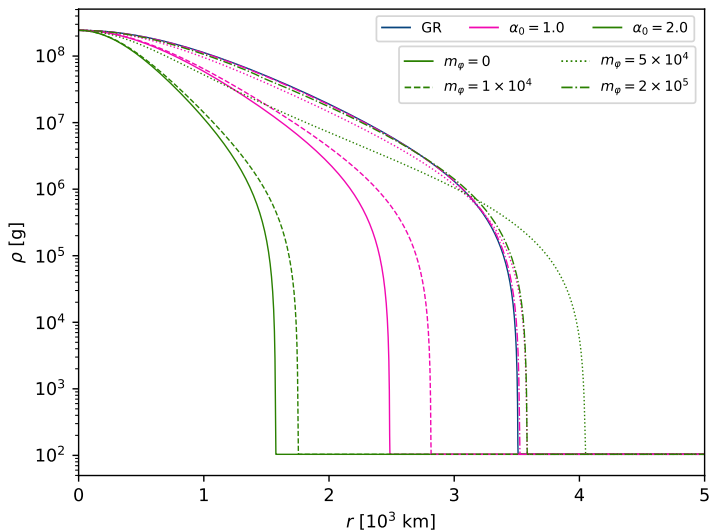

Figure 4. Radial density profile for $p_c = 7.2 \times 10^{25} \mathrm{g\,cm^{-1}s^{-2}}$.

Mass-Radius Relation

Numerical Results – Scalar Field profile

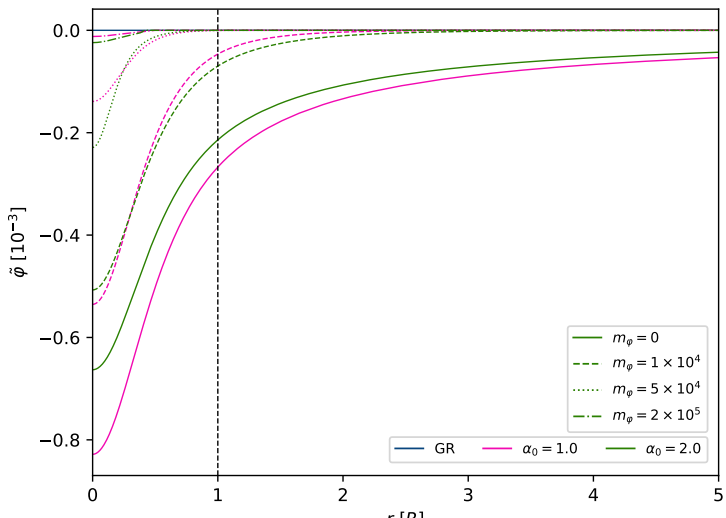

Figure 5. Radial scalar field profile for $p_c = 7.2 \times 10^{25} \mathrm{g\,cm^{-1}s^{-2}}$.

Part II

Cooling Process

Cooling Age

Cool down from $T(t = 0) = 10^8$K to $T(t_0) = 10^6$K

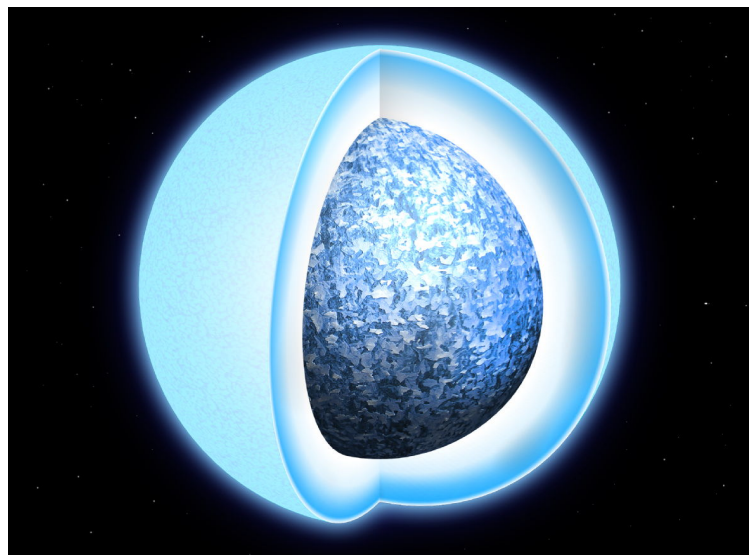

Figure 6. Artist's impression of a white dwarf star in the process of solidifying. Credit: University of Warwick, Mark Garlick

Cooling Process

Thermal Energy

- Luminosity by decrease of residual thermal energy

$$\boxed{L = -\frac{\mathrm{d}U}{\mathrm{d}t} = -\bar{c}_v \frac{M}{A m_p} \frac{\mathrm{d}T}{\mathrm{d}t}} \tag{8}$$

- Mean specific heat

$$\bar{c}_v = \frac{1}{M} \int_0^M \mathrm{d}m \left(c_v^{\mathrm{el}} + c_v^{\mathrm{ion}} \right) \tag{9}$$

- Specific heat of electrons per ion

$$c_v^{\mathrm{el}} = \frac{3}{2} \frac{k_B \pi^2}{3} Z \frac{k_B T}{\epsilon_F} \tag{10}$$

- Specific heat of ions

$$\Gamma < \Gamma_m : \quad c_v^{\mathrm{ion}} = \frac{3}{2} k_B \,, \tag{11}$$

$$\Gamma \geq \Gamma_m : \quad c_v^{\mathrm{ion}} = \frac{9 k_B}{y^3} \int_0^y \mathrm{d}x \frac{x^4 e^x}{(e^x - 1)^2} \,, \quad y := \Theta_D / T \tag{12}$$

$$\Theta_D = 0.174 \times 10^4 \frac{2Z}{A} \sqrt{\rho}$$

Constants: mean atomic weight A, charge Z; variables: Fermi energy ϵ_F, Debye temperature Θ_D

Cooling Process

Thermal Energy – Specific Heat

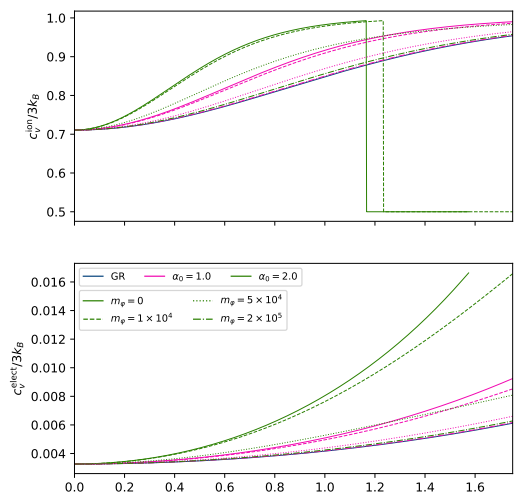

Figure 7. Specific heat of ions (upper) and electrons (lower panel) at temperature $T = 10^7$ K with $\Gamma_m = 60$ for a WD with $p_c = 1.5 \times 10^{26}\ \mathrm{gcm^{-1}s^{-2}}$.

Cooling Process

Thermal Energy – Mean Specific Heat

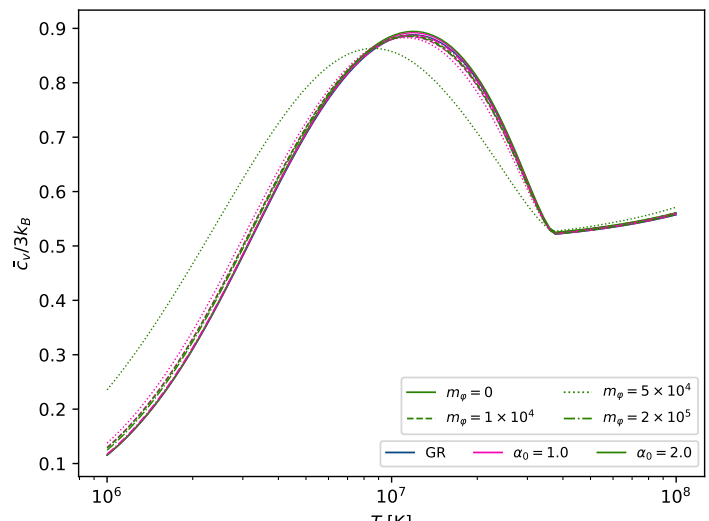

Figure 8. Mean specific heat for scalar-tensor theories and GR with $\Gamma_m = 60$ for a WD with $p_c = 1.5 \times 10^{26}$ gcm^{-1}s^{-2}.

Cooling Process

Crystallization

- Liquid to solid phase transition at the center

$$\Gamma = 2.28 \times 10^5 \frac{Z^2}{T} \left(\frac{\rho}{A}\right)^{1/3}, \quad \Gamma_m \in \{60, 125\}$$

- Additional energy loss through latent heat qk_BT

$$L_q = qk_BT \frac{\mathrm{d}}{\mathrm{d}t}\left(\frac{m_s}{Am_p}\right) = \frac{qk_BT}{Am_p}\frac{\mathrm{d}m}{\mathrm{d}r}\frac{\mathrm{d}r}{\mathrm{d}\rho}\frac{\mathrm{d}\rho_s}{\mathrm{d}T}\frac{\mathrm{d}T}{\mathrm{d}t} \tag{13}$$

- At critical point Γ_m

$$\boxed{L_q = 3\rho_s qk_B \frac{M}{Am_p}\frac{1}{M}\left[\frac{\mathrm{d}m}{\mathrm{d}r}\frac{\mathrm{d}r}{\mathrm{d}\rho}\right]_{r=r_s}\frac{\mathrm{d}T}{\mathrm{d}t}} \tag{14}$$

- Total core luminosity: thermal energy (8) and latent heat (14)

$$L_{\text{core}} = \frac{3k_BM}{Am_p}\left(\frac{\rho_s q}{M}\left[\frac{\mathrm{d}m}{\mathrm{d}r}\frac{\mathrm{d}r}{\mathrm{d}\rho}\right]_{r_s} - \frac{\bar{c}_v}{3k_B}\right)\frac{\mathrm{d}T}{\mathrm{d}t} \tag{15}$$

Boltzmann constant k_B, charge Z, mean atomic weight A, numerical constant q, proton mass m_p.
Crystallized energy density $\rho_s(T)$, crystallized mass m_s, radius r_s for which $\rho(r_s) = \rho_s(T)$.

Cooling Process

Surface Layer Structure

- Nondegenerate surface layers

$$L = -4\pi\tilde{r}^2 \frac{c}{3\kappa\tilde{\rho}} \frac{\mathrm{d}}{\mathrm{d}\tilde{r}} \left(aT^4\right) \ . \tag{16}$$

- Kramer's opacity $\kappa = \kappa_0 \rho T^{-3.5}$

$$\frac{\mathrm{d}p}{\mathrm{d}T} = \frac{4\pi G m}{3LA^4(\tilde{\varphi})\kappa_0} \frac{4ac}{\mu m_u} \frac{k_\mathrm{B}}{\mu m_u} \left\{ \tilde{r}^2 c^2 \left(\alpha\tilde{\varphi}' + \frac{\tilde{r}\tilde{\varphi}'^2}{2}\right) \left(1 + \frac{\tilde{r}^3 c^2}{4Gm} V(\tilde{\varphi})\right) \left(1 - \frac{2Gm}{\tilde{r}c^2}\right)^{-1} \right\} \frac{T^{6.5}}{p} \ . \tag{17}$$

- Density ρ_* and temperature T_* at the transition layer

$$\frac{\rho_* k_B T_*}{\mu_e m_u} = 10^{13} \left(\frac{\rho_*}{\mu_e}\right)^{5/3} \tag{18}$$

- Surface layer luminosity with $C \approx 2 \times 10^6$ ergs^{-1}K$^{-3.5}$

$$\boxed{L_{\mathrm{STT}} = \frac{C}{A^4(\tilde{\varphi}_s)} \left\{ \frac{\tilde{r}_s^2 c^2}{GM} \left(\alpha\tilde{\varphi}_s' + \frac{\tilde{r}_s \tilde{\varphi}_s'^2}{2}\right) \left(1 + \frac{\tilde{r}_s^3 c^2}{4GM} V(\tilde{\varphi}_s)\right) \left(1 - \frac{2GM}{\tilde{r}_s c^2}\right)^{-1} \right\} \frac{M}{M_\odot} T_*^{3.5}} \tag{19}$$

Constants: Boltzmann constant k_B, mean molecular weight μ, atomic mass unit m_u, gravitational constant G, radiation constant a, Kramer's opacity constant κ_0

Cooling Process

Cooling Age

- Total core luminosity

$$L_{\text{core}} = \frac{3k_B M}{Am_p}\left(\frac{\rho_s q}{M}\left[\frac{\mathrm{d}m}{\mathrm{d}r}\frac{\mathrm{d}r}{\mathrm{d}\rho}\right]_{r_s} - \frac{\bar{c}_v}{3k_B}\right)\frac{\mathrm{d}T}{\mathrm{d}t} \tag{20}$$

- Surface layer luminosity

$$L_{\text{surf}} = \frac{C}{A^4(\tilde{\varphi}_s)}\left\{\frac{\tilde{r}_s^2 c^2}{GM}\left(\alpha\tilde{\varphi}_s' + \frac{\tilde{r}_s\tilde{\varphi}_s'^2}{2}\right)\left(1 + \frac{\tilde{r}_s^3 c^2}{4GM}V(\tilde{\varphi}_s)\right)\left(1 - \frac{2GM}{\tilde{r}_s c^2}\right)^{-1}\right\}\frac{M}{M_\odot}T_*^{3.5} \tag{21}$$

- Integrate numerically to obtain cooling age

Boltzmann constant k_B, charge Z, mean atomic weight A, numerical constant q, proton mass m_p.
Crystallized energy density $\rho_s(T)$, crystallized mass m_s, radius r_s for which $\rho(r_s) = \rho_s(T)$.

Cooling Process

Cooling Age

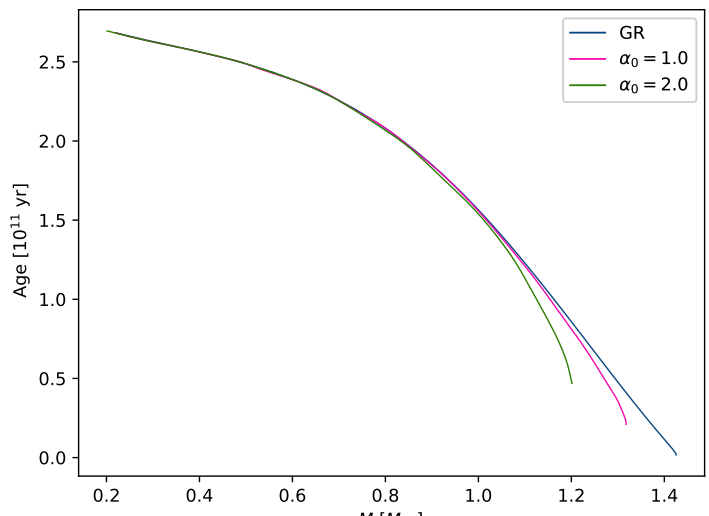

Figure 9. Cooling age of WD with crystallization for scalar-tensor theories with scalar field mass $m_{\tilde{\varphi}} = 2 \times 10^5$ and GR for $\Gamma_m = 60$.

Conclusions & Outlook

- Massive Brans-Dicke theory
  - Reduces Chandrasekhar mass limit for WD
  - Affects internal stellar properties
  - Shortens cooling time and thus cooling age
- Future improvements
  - Salpeter equation of state
  - More realistic cooling model
- Oscillations

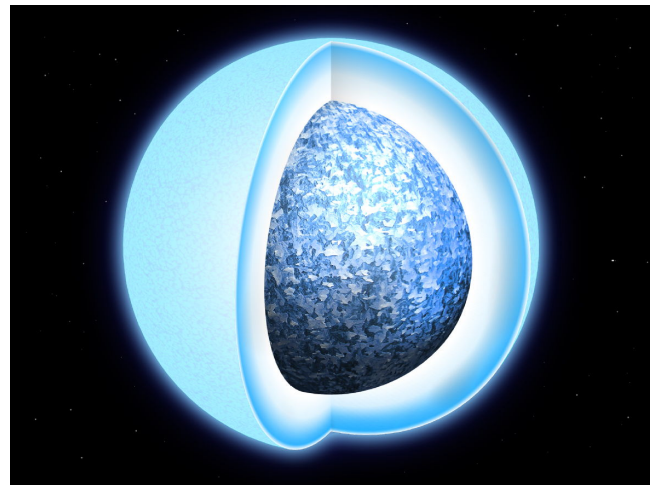

Figure 10. Artist's impression of a white dwarf star in the process of solidifying. Credit: University of Warwick, Mark Garlick

References

- Brush, SG, HL Sahlin, and E Teller (1966). **"Monte Carlo Study of a One-Component Plasma. I".** In: *The Journal of Chemical Physics* 45.6, pp. 2102–2118.
- Chandrasekhar, S. (Jan. 1935). **"The Highly Collapsed Configurations of a Stellar Mass. (Second Paper.)".** In: *Monthly Notices of the Royal Astronomical Society* 95.3, pp. 207–225. ISSN: 0035-8711. DOI: 10.1093/mnras/95.3.207.
- Kalita, Surajit and Banibrata Mukhopadhyay (2019). **"Continuous gravitational wave from magnetized white dwarfs and neutron stars: possible missions for LISA, DECIGO, BBO, ET detectors".** In: *Monthly Notices of the Royal Astronomical Society* 490.2, pp. 2692–2705.
- Saumon, Didier, Simon Blouin, and Pier-Emmanuel Tremblay (2022). **"Current challenges in the physics of white dwarf stars".** In: *Physics Reports* 988, pp. 1–63.
- Shapiro, Stuart L and Saul A Teukolsky (2008). ***Black holes, white dwarfs, and neutron stars: The physics of compact objects.*** John Wiley & Sons.
- Tremblay, Pier-Emmanuel et al. (Jan. 2019). **"Core crystallization and pile-up in the cooling sequence of evolving white dwarfs".** In: 565.7738, pp. 202–205. DOI: 10.1038/s41586-018-0791-x. arXiv: 1908.00370 [astro-ph.SR].
- Van Horn, HM (1968). **"Crystallization of white dwarfs".** In: *Astrophysical Journal, vol. 151, p. 227* 151, p. 227.

Evolutionary Tracks

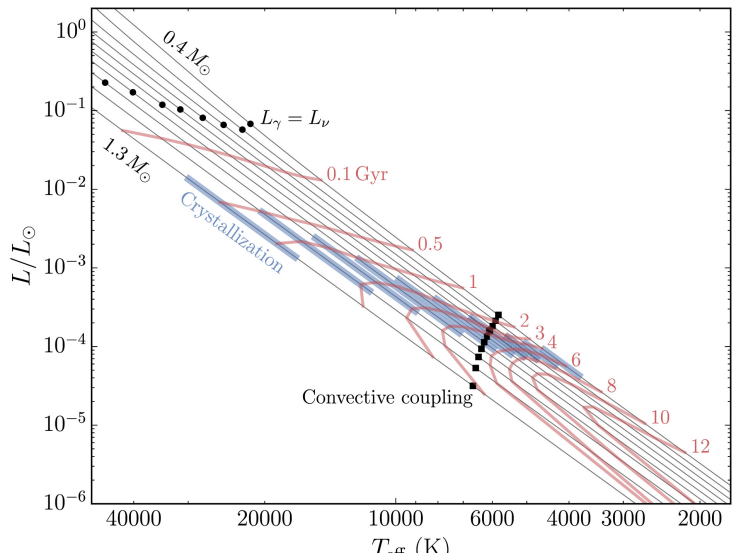

Figure 11. Evolutionary tracks (gray lines) of C–O core DA white dwarf models. Depicted are the isochrones (red curves), transition between neutrino and thermal cooling (filled circles), core crystallization (blue sections) and onset of convective coupling (squares). Taken from Saumon, Blouin, and Tremblay 2022.

Mass-Density Relation

Numerical Results for Newtonian Gravity and GR

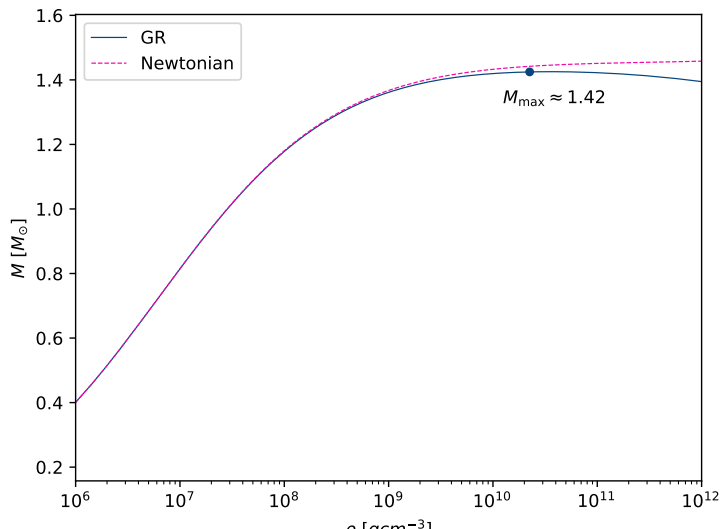

Figure 12. Mass-density relation for GR and Newtonian Gravity.

Mass-Density Relation

Numerical Results for STT

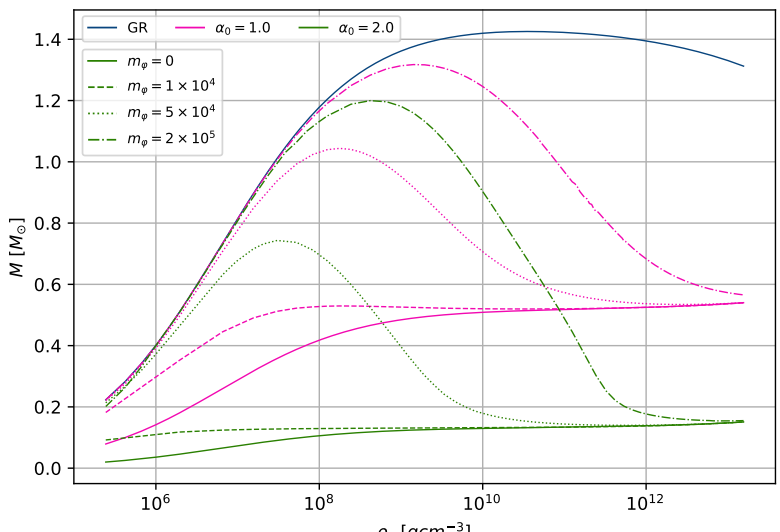

Figure 13. Mass-density relation.

Mass-Density Relation

Numerical Results for STT – Scalar Field

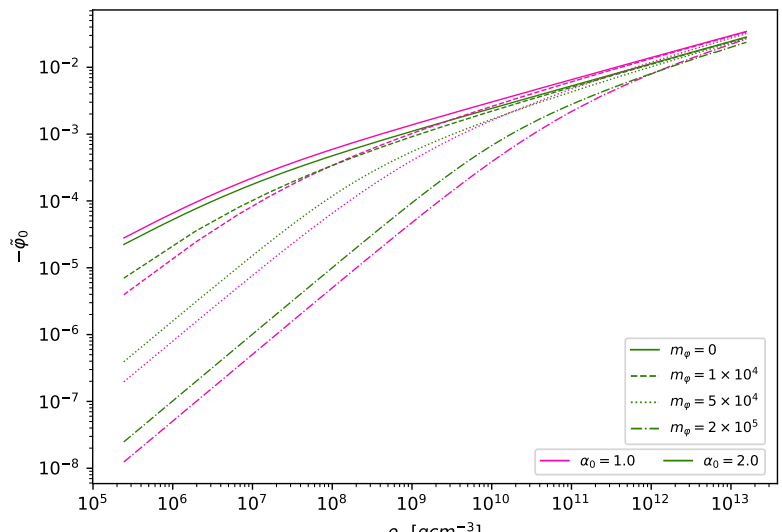

Figure 14. Numerically obtained central values for the scalar field.

Cooling Process

Cooling Age in Newtonian Gravity and GR

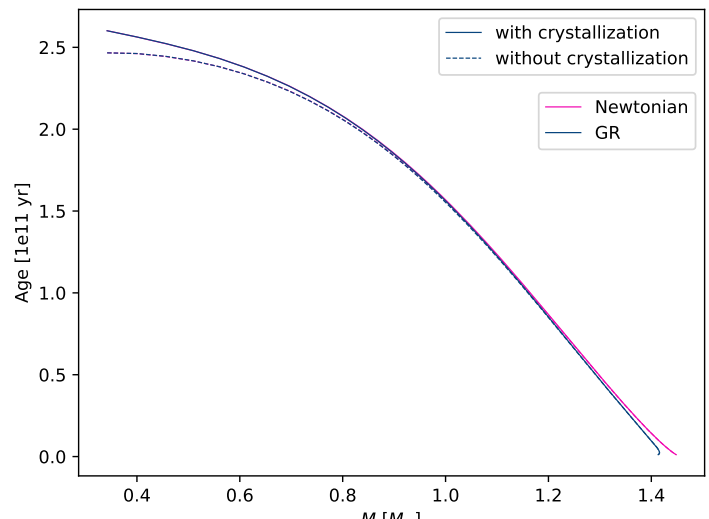

Figure 15. Cooling age of WD with and without crystallization for GR and Newtonian Gravity with $\Gamma_m = 60$.